Applied Cardiopulmonary Pathophysiology 14: 229-235, 2010

Influence of capillary geometry on hypoperfusion-induced ischemia: a numerical study

F. Jung[1], G. Pindur[2], B. Hiebl[1], R. P. Franke[3]

[1]Centre for Biomaterial Development and Berlin-Brandenburg Center for Regenerative Therapies (BCRT), Institute for Polymer Research, Helmholtz Zentrum für Material- und Küstenforschung, Teltow, Germany; [2]Institute of Clinical Haemostasiology and Transfusion Medicine, University of Saarland, Homburg, Germany; [3]Central Institute for Biomedical Engineering, Department of Biomaterials, University of Ulm, Germany

Abstract

Under physiological conditions, tissue oxygen tension depends mainly on oxygen convection in the flowing blood and on oxygen consumption of the cells in the surrounding tissue. Below a certain limit velocity, 50 % of the cells in a Krogh cylinder do not receive enough oxygen to survive and cell death may occur. For a given capillary geometry, such a limit velocity can be calculated by finding numerical solutions to coupled partial differential equations.
The results show that the risk of tissue ischemia depends very strongly on capillary architecture and the velocity of capillary blood flow. When capillary erythrocyte velocity falls below 0.26 mm/s, there will be an insufficient blood supply to the region supplied by the distal venous branch of a capillary of 1 mm length, whereas in short capillaries this will occur only when velocities fall below 0.024 mm/s.
It seems that regions with a high metabolic demand, for example the retina or the myocardium, have short capillaries with rapid blood flow. This means that they have a greater blood flow reserve before an ischemic event can occur.

Key words: capillary dimension, ischemia, hypoperfusion

1. Introduction

Material exchange and thus oxygen supply to tissue cells – without which cells could not survive – as well as disposal of metabolic intermediates and end products from tissues takes place in the terminal capillary network. This network comprises the precapillary arterioles, the capillary bed and the post-capillary venules. Oxygen exchange takes place via diffusion. Oxygen is bound to haemoglobin in the erythrocytes and is transported by convection through the arterial blood stream from the lungs to the capillary network. The respective area of exchange (approx. 300 m^2) resulting from the extremely high number of capillaries – approx. 8 to 10 billion – is so large that the oxygen supply is not limited by diffusion but by convective transport of oxygen (circulation-limited oxygen exchange).

Local tissue oxygen tension thus primarily depends on the delivery of oxygen by circulating blood (but also on diffusion if the diffusion process through the vessel wall and into the tissue is impaired) and on the oxygen consumption of tissue cells [13, 22]. A minimum velocity of the oxygen-transporting erythrocytes in capillaries is required to supply

enough oxygen to the tissue, below which approximately 50 % of the surrounding tissue region (Krogh cylinder [18]) would be undersupplied with oxygen, resulting in a higher risk of cell deaths. Cell death occurs when the oxygen partial pressure in the tissue falls below 0.05 mmHg [26]; for mitochondria the critical oxygen partial pressure is 0.01 mmHg [3, 26].

For a given capillary geometry, a limit velocity can be calculated by the numerical solution for mass and impulse transport, below which ischemic regions in the tissue surrounding a capillary can occur.

2. Methods

Mathematical formulation

Figure 1 shows a Krogh cylinder model. This is the cylindrical tissue region (with radius rT) surrounding a capillary (with a capillary radius rC) from which it is supplied [17] (see Figure 1).

The partial differential equation for a capillary (Equation 1) using cylinder coordinates [7] that describes the physical process of supplying oxygen to the tissue is:

$$\frac{\delta^2 p}{\delta x^2} + \frac{\delta^2 p}{\delta r^2} + \frac{\delta p}{r\ \delta r} - \frac{v(r)}{D1}$$

$$\left[1+s(p) * \frac{b_s}{C1 * p}\right] \frac{\delta p}{\delta x} = 0$$

where:

p:	oxygen partial pressure
v(r):	velocity field
s(p):	oxygen binding curve
bs:	max. O_2 concentration in blood
D1:	O_2 diffusion coefficient for blood
C1:	O_2 solubility in blood

and for the surrounding tissue (Equation 2):

$$\frac{\delta^2 p}{\delta x^2} + \frac{\delta^2 p}{\delta r^2} + \frac{\delta p}{r\ \delta r} - \frac{A(p)}{D2 * C2} = 0$$

where:

A(p):	oxygen consumption in tissue
D2:	O_2 diffusion coefficient in tissue
C2:	O_2 solubility in tissue

With the following boundary and initial conditions:

$$p(x=0,\ r<r_c) = p_0$$

$$\frac{\delta p(r=0.x)}{\delta r} = 0$$

$$\frac{\delta p(r=rT,\ x)}{\delta r} = 0$$

$$\frac{\delta p(r>r_c,\ x=0)}{\delta x} = 0$$

$$\frac{\delta p(r>r_c,\ x=xE)}{\delta x} = 0$$

and the following transition condition (Equation 3

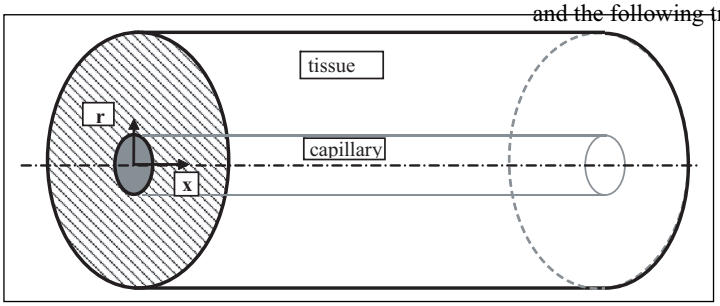

Figure 1. Krogh cylinder model

and the following transition condition (Equation 3):

$$C1 * D1 \frac{\delta p\,(x, r=r_k)}{\delta r} = C2 * D2 \frac{\delta p\,(x, r=r_k)}{\delta r}$$

this system of equations can be solved by approximation.

Numerical solution

It is not possible to obtain an analytical solution to this coupled system of second-order partial equations. In this study, a difference method was chosen to solve the model problem numerically. In the first step, the steady-state problem was discretised by superimposing a grid over the interval for which the differential equations and boundary conditions are valid. An equation now had to be formulated for each grid point. This can be achieved by substituting the differentials by difference quotients. This system of difference equations renders a value at each grid point dependent on neighbouring points. The transition equation (Equation 3) is used for the capillary region, the tissue region and the capillary border. In general, the resulting system of equations (in the case of small grid distances) is still too large. Thus, in order to be able to solve such discrete systems, an approximation procedure (here a relaxation procedure [28]) needs to be applied. To this end, the grid points are assigned starting values and all grid points are recalculated to give improved values. This iteration is repeated until a stable approximation of the solution is reached that satisfies the required accuracy. For each iteration step, the sum of corrections performed on all grid points as well as the value and location of maximum correction is stored and the convergence of the solution verified. The maximum correction value is used as the termination criterion.

A typical oxygen distribution in capillaries and the surrounding tissues is shown in Figure 2.

The capillary entry pressure is equal to the arterial pO_2. Through diffusion of oxygen into the tissue the arterial pO_2 is gradually reduced along the longitudinal capillary axis. Oxygen diffusing into the tissue also decreases due to oxygen consumption in the tissue. The lowest O_2 values are found at the border of the tissue cylinder region at the venous ends of the capillaries. This theoretical distribution of pO_2 in a Krogh cylinder model predicted by Ehrly was confirmed by intracuta-

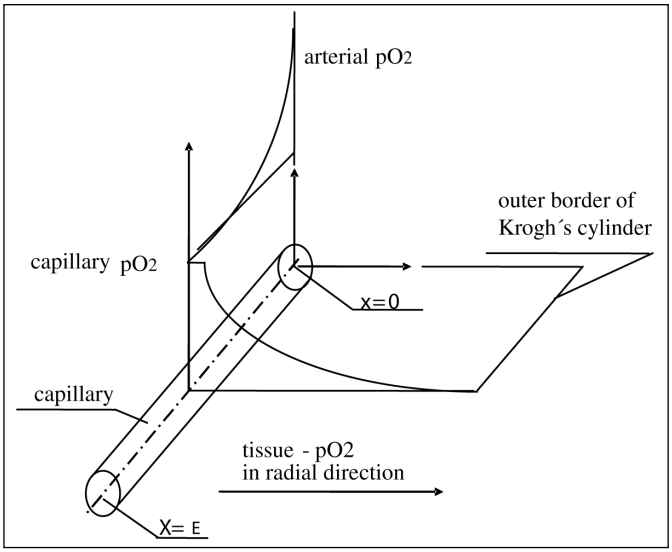

Figure 2: Schematic distribution of oxygen partial pressure in a capillary and the surrounding tissue (Krogh cylinder) according to Lübbers [15].

neous measurements of pO_2 profiles using pO2 microprobes.

Results

Figure 3 shows the percentage of adequate oxygenation of the Krogh tissue region for capillaries of different lengths (100, 200 and 1000 µm) as a function of perfusion velocity (0-300 [µm/s]). Tissue regions with oxygen partial pressures under 0.05 mmHg [26] are regarded as undersupplied. The following constants were used to solve the system of equations:

O_2 solubility in blood:
$C1 = 0.2112 \times 10^{-6}$ [mlO_2/g*Pa]

O_2 solubility in tissue:
$C2 = 0.1776 \times 10^{-6}$ [mlO_2/g*Pa]

Diffusion coefficients:
$D1 = D2 = 2300$ [$\mu m^2/s$]

O2 consumption rate in tissue:
A(p) = A0 if p > pG0
A0 x p/p x T0 otherwise

where: A0 = 0.0013 [mlO2/g*s]
pT0 = 7 Pa

Maximum O2 concentration in blood:
bs = 0.2144 [ml O_2/ml blood]

O_2 binding curve: $(\sum (i \times Ai \times p0i)) / (4 \times \sum (1 + Ai \times p0i))$ for i=1-4

where: p0 = 0.009 x p [Pa]
$A1 = 2.18 \times 10^{-2}$
$A2 = 9.12 \times 10^{-4}$
$A3 = 3.75 \times 10^{-6}$
$A3 = 2.47 \times 10^{-6}$

Figure 4 shows the influence of diffusion conditions due to changed tissue diffusion coefficients (between 1900 to 2500 $\mu m^2/s$) on tissue pO_2. A physiological tissue diffusion coefficient of 2300 $\mu m^2/s$ was assumed. A 31.5 % change affected tissue pO_2 by less than 0.5 mmHg at a distance of 40 µm from the capillary, which is minimal.

Discussion

Under physiological conditions, oxygen supply to the tissue depends on unimpaired regulation of capillary circulation, capillary geometry, capillary haematocrit, plasma viscosity, erythrocyte rigidity and oxygen consumption in the tissue [20, 22]. Figure 3 shows the considerable influence of capillary

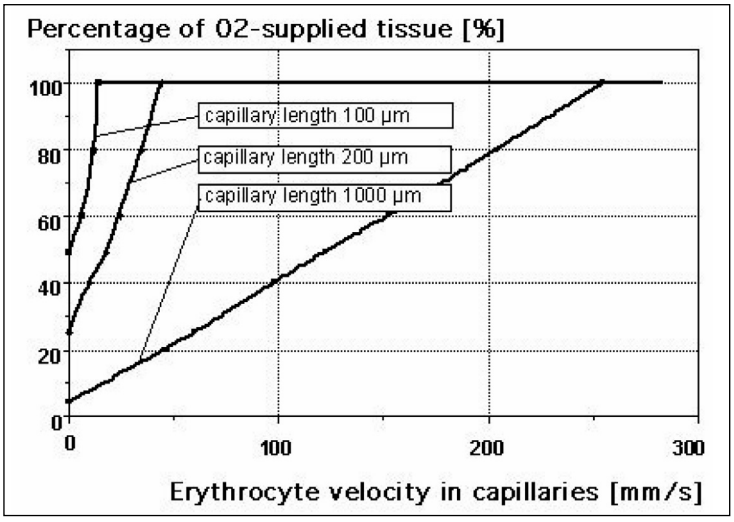

Figure 3: Influence of velocity and capillary length on oxygen partial pressure

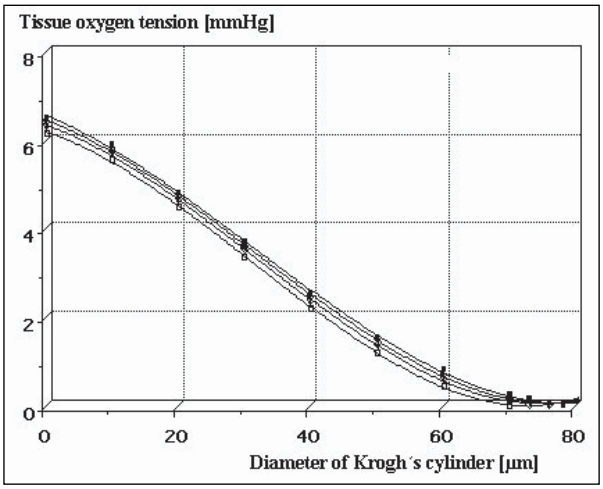

Figure 4: Tissue oxygen tension from the capillary wall to the border of the Krogh cylinder for four different diffusion coefficients (D1=1900, D2=2100, D3=2300, D4=2500 [µm²/s])

blood flow velocity on the proportion of insufficiently oxygenated tissue. The longer the capillary, the earlier will a reduction in capillary erythrocyte velocity result in an undersupply of oxygen to the surrounding tissue. For capillaries of 1 mm length (found in skin, where lengths of 3 mm [2] are reached), the first cells within the region of a distal venous capillary branch are undersupplied with oxygen at erythrocyte velocities of 0.26 mm/s, whereas in the case of short capillaries – as found in the peri-macular capillary network [1] – undersupply does not occur until velocities decrease to less than 0.02 mm/s. Furthermore, the short peri-macular capillaries in the retina are, on average, perfused more rapidly (about 3 times higher erythrocyte velocities under resting conditions) than the capillaries of the skin [10, 29]. Thus, the risk of tissue ischemia depends very strongly on capillary architecture and the velocity of capillary blood flow. The diffusion conditions in tissue play a secondary role (see Figure 4).

This observation on a singular capillary cannot be extrapolated to regions with complex microcirculation regulation [22]. In organs, capillary flow velocities are constant. Erythrocyte velocity in skin capillaries, for example, fluctuates 6 to 8 times per minute [24] with a variance of the mean of about 30 %. Very low mean capillary erythrocyte velocities have been observed in patients with autonomic microangiopathy and an underlying advanced atherosclerotic disease in combination with a lipid metabolic disorder or hypertension and/or diabetes mellitus [11, 12, 23]. Nevertheless, skin necroses normally do not occur. This could be due to the fact that, even in regions with microcirculation, regulative processes can occur which contribute to the redistribution of capillary flow. The research group headed by Lübbers [19] demonstrated on an animal model that in an organ with very inhomogeneous capillary lengths (100–550 mm), for example the kidney, microcirculation disorders induced pharmacologically or during ventilation hypoxia resulted in pO_2 reductions in regions with high tissue pO_2 values whereas in regions with low tissue pO_2 values (for example in the region around long sinusoids) these reductions were less marked [15, 27]). It was also shown that cells tolerated oxygen deficiency during minimum microcirculation as long as energy was provided via anaerobic glycolysis and elimination of the resulting protons from the tissue was adequate [9].

In contrast, when microcirculation stalled, lactic acidosis led to a rapid decrease in ATP [16] and, as a consequence, to severe cell damage even resulting within a few minutes in death (necrosis) of cells that have a high oxygen demand (e.g. nerve cells).

In summary, it thus seems that tissue regions with a high metabolic demand – for example in the retina and the myocardium [14] – are equipped with short capillaries to better cope with a temporarily insufficient or stagnating blood flow.

References

1. Arend O, Wolf S, Jung F, Bertram B, Pöstgens H, Toonen H, Reim M. Retinal microcirculation in patients with diabetes mellitus: dynamic and morphological analysis of perifoveal capillary network. Br J Ophthalmol 1991; 75 (9): 514-8
2. Cevc G, Vierl U. Spatial distribution of cutaneous microvasculature and local drug clearance after drug application on the skin. J Control Release 2007; 118 (1): 18-26
3. Chance B, Pring M. Logic in the design of the respiratory chain. In: B. Hess, H. Staudinger (Eds.) Biochemie des Sauerstoffs (pp. 102-126). Springer, Berlin, 1968.
4. Dold A, Eckmann B. Numerische Behandlung nichtlinearer Integrodifferential- und Differentialgleichungen. Springer Verlag, Berlin, 1973.
5. Grocott HP. Characteristics, incidence, and pathomechanisms of neurological damage during cardiac surgery. Applied Cardiopulmonary Pathophysiology 2009; 13: 20-26
6. Grossherr M, Bechtel JFM, Heinze H, Klotz K-F, Sievers H-H,Eichler W. Effects of pulmonary artery perfusion on gas exchange and alveolar matrix metalloproteinases after cardiopulmonary bypass in a swine model. Applied Cardiopulmonary Pathophysiology 2009; 13: 123-129
7. Grossmann U. Mathematische Grundlagen der Sauerstoffversorgung von Warmblüterorganen. Dissertationsschrift, Ruhruniversität Bochum, 1979
8. Hiebl B, Müller C, Jung F, Hünigen H, Hamm B, Plendl J, Niehues SM. Macro- and micromorphometric studies of the vascular structures from the Göttingen® minipig. Applied Cardiopulmonary Pathophysiology 13: 318-321
9. Höper J, Kessler M, Starlinger H. Preservation of ATP in the perfused liver. In: H.I. Bicher, D.F. Bruley (Eds.) Oxygen Transoprt to Tissue (pp. 371-375). Plenum Publishing Corp., New York, 1973
10. Jung F, Wappler M, Nüttgens HP, Kiesewetter H, Wolf S, Müller G. Method of video capillary microscopy: determination of geometric and dynamic measuring parameters. Biomed Tech (Berl) 1987; 32 (9): 204-13
11. Jung F, Kolepke W, Spitzer S, Kiesewetter H, Ruprecht KW, Bach R, Schieffer H, Wenzel E. Primary and secondary microcirculatory disorders in essential hypertension. Clin Investig 1993; 71: 132-138
12. Jung F, Mrowietz C, Labarrere C, Schüler S, Park J.-W. Primary cutaneous microangiopathy in heart recipients. Microvasc Res 2001; 62: 154-163
13. Jung F. From hemorheology to microcirculation and regenerative medicine: Fåhraeus Lecture 2009. Clin Hemorheol Microcirc 2010; 45: 79-99
14. Kassab G.S., Fung YC. Topology and dimensions of pig coronary capillary network. Am J Physiol 1994; 267 (1 Pt 2): H319-25
15. Kessler M, Schmeling D. Methodology of pH sensitive microelectrodes for intracellular measurements. Pflügers Arch 1973; 343: 128
16. Kessler M, Höper J, Schäfer D, Starlinger H. Sauerstofftransport im Gewebe. In: F.W. Ahnefeld, C. Burri, W. Dick, M. Halmagyi (Eds.) Mikrozirkulation (pp. 36-52). Springer, Berlin, 1974
17. Krogh A. The Anatomy and Physiology of Capillaries. Yale University Press, Newhaven, 1922
18. Krogh A. The number and distribution of capillaries in muscles with calculations of the oxygen pressure head necessary for supplying the tissue. J of Physiol 1919; 52: 405
19. Lübbers DW. Quantitative measurement and description of oxygen supply to the tissue. In: Jöbsis F.F. (Ed.) Oxygen and Physiological Function (p. 254). Professional Information Library, Dallas, 1977
20. Marossy A, Svorc P, Kron I, Gresová S. Hemorheology and circulation. Clin Hemorheol Microcirc 2009; 42 (4): 239-58
21. Marsal D. Die numerische Lösung partieller Differentialgleichungen. B.I. Wissenschaftsverlag, 1976
22. Matschke K, Jung F. Regulation of the myocardial microcirculation. Clin Hemorheol Microcirc 2008; 39; 265-279

23. Park JW, Mrowietz C, Schüler S, Labarrere C, Jung F. Cutaneous microcirculation in cardiac allograft recipients with severe hypercholesterolemia before, during, and after the first HELP apheresis. Applied Cardiopulmonary Pathophysiology 2000; 9: 19-25
24. Salerud EG, Tenland T, Nilsson GE et al. Rhythmical variations in human skin blood flow. Int J Microcirc Clin Exp 1983; 2: 91-102
25. Schmid-Schönbein H. Microrheology of erythrocytes, blood viscosity, and the distribution of blood flow in the microcirculation. In: A.C. Guyton, A.E. Cowley (Eds.) Int. Rev. Physiol. Cardiovascular Physiology II, Vol. 9. University Park Press, Baltimore, 1979
26. Starlinger H, Lübbers DW. Polarographic measurements of the oxygen pressure performed simultaneously with optical measurements of the redox state of the respiratory chain in suspensions of mitochondria under steady state conditions at low oxygen tension. Pflügers Arch 1973; 341: 15
27. Suwa N, Takahashi T. Morphological and morphometrical analysis of circulation in hypertension and ischemic kidney (ed. F. Büchner). Urban & Schwarzenberg, München, 1971
28. Törnig W. Numerische Mathematik für Ingenieure und Physiker. Springer, Berlin, 1979
29. Wolf, S, Toonen, H, Arend, O, Jung, F, Kaupp, A, Kiesewetter, H, Meyer-Ebrecht, D, Reim, M. Zur Quantifizierung der retinalen Kapillardurchblutung mit Hilfe des Scanning-Laser-Ophthalmoskops. Biomed Technik 1990; 35: 131-134

Correspondence address:
Prof. Friedrich Jung, M.D.
Center for Biomaterial Development and Berlin-Brandenburg Center for Regenerative Therapies (BCRT)
Helmholtz-Zentrum Geesthacht
Centre for Materials and Costal Research
Kantstr. 55
14513 Teltow
Germany
friedrich.jung@gkss.de